Pixel Apodization for the Suppression of Higher Diffractive Orders in Computer Holography

Joanna Starobrat and Michal Makowski
Faculty of Physics, Warsaw University of Technology, ul. Koszykowa 75, 00-662 Warsaw, Poland

Keywords: Computer-generated Holography, Higher Diffraction Orders, LCoS Spatial Light Modulator, Pixel Apodization.

Abstract: Demand for a next generation of head-up displays have increased the demand for the applicable holographic displays. From the available spatial light modulators (SLM), Liquid Crystal on Silicon (LCoS) SLMs are the most popular for the simplicity of addressing and their relatively low costs. However, improving its efficiency demands reduction of higher diffraction orders. In this work we propose a new solution, that is the pixel apodization as the means to redirect the light intensity from the undesirable images to the main image. The higher diffraction orders are the result of the rectangular shape of the pixels of the SLM, as it can be concluded from the Fourier Transform (FT) analysis. Hence we exploit the known property that a Gaussian function is, up to a constant multiple, its own FT. The presented simulations support the theoretical conclusions, as the apodization allows for a significant lowering of the intensity of the third and higher diffraction orders, in the same time increasing the intensity directed to the main image.

1 INTRODUCTION

Holography as an imaging technique has been known since the first half of XIX century (Gabor, 1949), with its theoretical background dating as early as 1920 (Wolfke, 1920). Being a method which allows reconstruction of not only amplitude, but also phase of the saved image, it has soon found its application in a wide range of fields, starting from simple three-dimensional image reconstruction (Denisiuk, 1978), going through beam-shaping (Meltaus et al., 2003), i.e. in particle-trapping (Reicherter et al., 1999), telecommunication (Parker et al., 1997) or medicine (West, 1976), ending with a modern idea of a holographic memory of high security (Betin et al., 2013).

In the modern days the demand for a next generation of displays has been increasing. The head-up displays are an especially pursued subject, which is one of the main reason for further development of applicable holographic displays. Among the advantages offered by this technology, creating a real 3D images, low intensity-to-heat conversion and uncomplicated set-up of few elements can be named (Slinger et al., 2005).

Though many different types of spatial light modulators (SLM) are used in order to change the amplitude and/or phase of the wavefront (Casasent, 1977), the liquid crystal on silicon (LCoS) are considered the most popular due to their diffraction efficiency, simplicity of pixel addressing and relatively low costs (Michakiewicz and Kujawiska, 2009). The LCoS SLMs technology is still, however, facing challenges that remain to be overcome. While the pixel size is limited by the production machinery and the crosstalk between single liquid crystal cells occurs (Yang et al., 2013), another issue has been chosen as the main subject of our research, and that is the presence of images in higher diffractive orders (Makowski et al., 2012; Yaras et al., 2010). The state of art technology employs spatial filtering as the method of reducing the influence of the undesired images (Agour et al., 2009). This approach allows to eliminate higher diffraction orders, however, it largely decreases the intensity of the final wavefront while also presenting difficulties with successful filtering of the highest diffraction orders.

In this paper we conclude that the higher diffraction orders visible in a reconstruction of computer-generated Fourier hologram are the result of the rectangular shape of the pixels. This judgement is based on the analysis of both theory of the reconstruction of the said type of a hologram, and known Fourier transforms. Rectus function subjected to the FT results in a sinc function (Kreyszig, 1988), characterised by

Starobrat, J. and Makowski, M.
Pixel Apodization for the Suppression of Higher Diffractive Orders in Computer Holography.
DOI: 10.5220/0006551901600165
In *Proceedings of the 6th International Conference on Photonics, Optics and Laser Technology (PHOTOPTICS 2018)*, pages 160-165
ISBN: 978-989-758-286-8
Copyright © 2018 by SCITEPRESS – Science and Technology Publications, Lda. All rights reserved

multiple extrema in the spectrum. Thus, we propose the effective change of the shape of pixels. As it is known, a Gaussian function is, up to a constant multiple, its own Fourier transform. We propose a change of the pixel shape from rectus to a Gaussian function in order to avoid the multiple maxima of the intensity visible in the image reconstruction. Seeing as the LCoS SLM production is limited by the LCD technology capabilities, changing not physical, but effective shape of the single SLM cells would be advisable. In our research we employ amplitude masks as the means of altering the SLM effective structure.

2 PROPOSED METHOD

The high time-consumption and cost of employing the suggested solution in an experiment led to a decision of preparing and analysing simulations before conducting the experiment itself. In the next sections the assumptions made for the theoretical model of the hologram reconstruction are explained. In this research, LightSword software was used, which enables the simulation and numeric analysis of wavefronts propagation.

2.1 Simulated Set-up

A very simple set-up was chosen for the simulation of image reconstruction from Fourier holograms, as can be seen in Figure 1. He-Ne laser ($\lambda = 632.8\ nm$) serves as a light source, while a half-plate is used to set proper polarisation in respect to the SLM. The lens enables the reconstruction of the image in its focal plane after wavefront reflects from the spatial light modulator. Thanks to the beamsplitter, observing the resulting intensity pattern to the side from the optical axis of the set-up is possible.

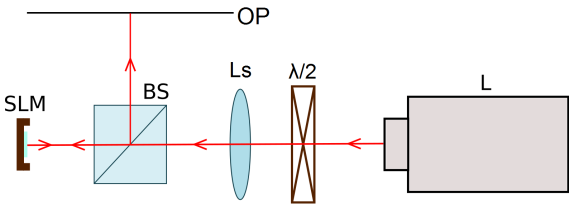

Figure 1: A schematic diagram of a simulated experimental set-up, where: L - He-Ne laser, λ/2 - half-wave plate, Ls - lens, BS - beamsplitter, SLM - spatial light modulator, OP - observation plane positioned in the focal distance from the lens.

2.2 SLM Structure

In the simulations, an SLM of HoloEye Pluto type was imitated as an amplitude distribution presented in a numeric array. Said model is characterized by the pixel size of 8 μm and the fill factor estimated as 93%, which implies the presence of spacing between single pixels. It is caused by fabrication limitations and needs to be considered in the theoretical model. Despite the resolution of 1920 x 1080 pixels of the SLM, only a matrix of 128 by 128 pixels was considered to simplify the simulations. To observe the effects of the apodization, oversampling was applied. This means that a square of 16 by 16 sampling points corresponded to a single SLM pixel and the final array size was 2048 by 2048. Such structure was approximated as a rectangular lattice consisting of squares with 7 μm sides and 1 μm spacing between them. A visualised fragment of a created structure is presented in the Figure 2.

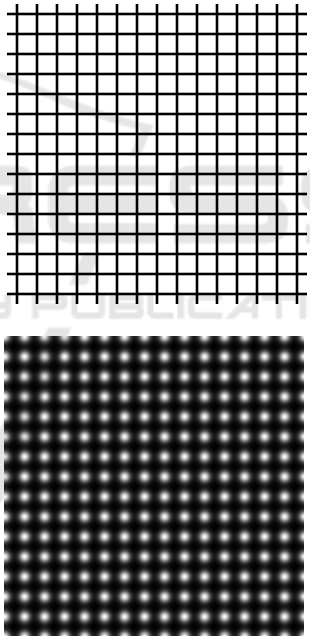

Figure 2: Fragments of the simulated structures. Top: amplitude distribution of the SLM pixel structure. Bottom: amplitude distribution of the Gaussian mask.

2.3 Masks Generation

As mentioned in the previous sections, a Gaussian shape of the pixels was proposed as a solution to the intensity leakage to the higher diffraction orders. The change of the effective pixel shape implies that each pixel needs to be apodized with a required function. For that reason, a lattice of desired elements had to be generated. In this case, the Gaussian functions of

a set radius were applied. A range of different radii values were considered, spanning from $w_1 = 4\ \mu m$, through $w_2 = 3.5\ \mu m$ and $w_3 = 3\ \mu m$, to $w_4 = 2.5\ \mu m$. Like in the case of the SLM structure, oversampling was applied and the same size of an array was used (2048 x 2048).

Bottom part of Figure 2 shows a fragment of the amplitude mask structure of $w_4 = 2.5\ \mu m$. Notably, centres of each square pixel and each Gaussian function were aligned for correct apodization.

The postulated Gaussian shape of the pixels might not be the optimal solution. Not only is it possible for another, more efficient mask to exist, but the difficulty of practical application is also an influential factor. For that reason a sinusoidal amplitude mask was simulated and analysed alongside the Gaussian masks. The period of the sinusoid function was matched to the pixel period of the SLM structure.

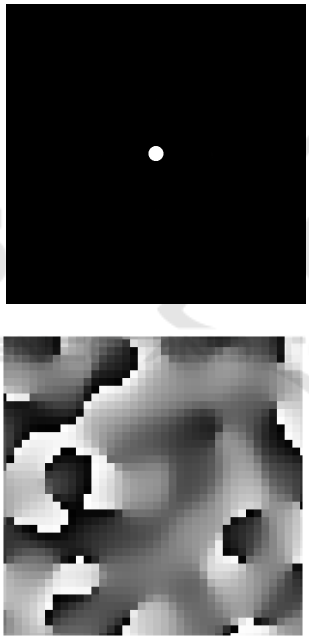

Figure 3: Computer-generated Fourier hologram. Top: simulated image. Bottom: fragment of the phase distribution of the hologram.

2.4 Fourier Hologram

Fourier hologram is a unique type of a hologram because of it saving the Fourier spectrum of the recorded image. The image can be reconstructed, as in the set-up shown on Figure 1, by a convergent spherical wave. In a computer-generated hologram, a Fourier transform of the simulated wavefront is calculated. Then, it is presented in an array of values corresponding to the phase change that is necessary to create a desired distribution.

A simulation utilizing a simple image of a small circle (Figure 3) was chosen to be presented in this paper due to the simplicity of obtained results and their viable analysis. A hologram of a size 128 by 128 pixels was generated, and only then it was rescaled to match the matrices prepared in the previous sections, that is to the size of 2048 x 2048. This allowed a uniform distribution of phase in the areas corresponding to single SLM pixels, which were set to have a side of 16 pixels.

3 SIMULATIONS

In order to conduct the simulations, all elements whose generation was described in the previous section must be combined. The SLM structure was first merged with the Fourier hologram phase distribution, and then mathematically multiplied by the amplitude mask as to simulate the apodization. While all the generated masks were applied, also a case of unapodized spatial light modulator was studied as the reference for further results. It should be noted that the zeroth diffraction order, present in the experimental hologram reconstruction, was not simulated, as the crosstalk effect between the pixels was omitted in the theoretical model.

The obtained wavefront amplitude distributions were analysed by two different methods. First of them was based on the visual presentation of the simulation results. Even though the differences between the obtained images were noticeable with bare eyes, the cross-sections of the distributions were calculated for improved assessment of the effectiveness of apodization. Figure 4 presents the examples of the acquired images and the cross-sections for the cases of no apodization, as well as Gaussian masks of $w_1 = 4\ \mu m$ and $w_4 = 2.5\ \mu m$.

The visual judgement is known to be insufficient as the means of theory evaluation, therefore the numerical results were also analysed and are demonstrated in the Tables 1 and 2. The values were obtained by the integration of the selected areas of first, second, as well as joint third and fourth orders of diffraction. The results shown in the Table 1 present the percentage of the amplitude distribution in each examined case separately, while in Table 2 normalized percentage distribution of amplitude can be found. The values given in the tables do not total up to 100%, as as the diffractive orders higher than fourth were not included.

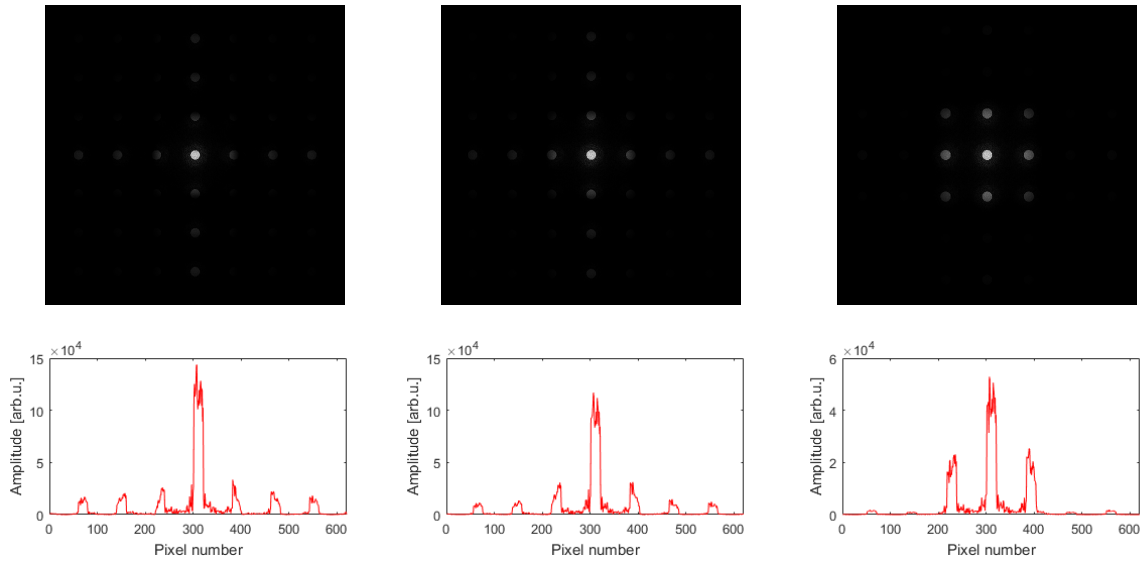

Figure 4: Amplitude of the image reconstructions from simulated holograms and the cross-sections of their distributions. Left: image obtained with an un-apodized spatial light modulator. Center: image obtained with the use of a first examined Gaussian mask, $w_1 = 4\ \mu m$. Right: image obtained with the use of a last examined Gaussian mask, $w_4 = 2.5\ \mu m$.

4 DISCUSSION

The visual results are rather simple to analyse, as the difference in hologram reconstructions is rather noticeable. Both Gaussian masks, including the one of the highest Gaussian diameter, redirects light into the main image, which corresponds to the first diffraction order. Said effect is more visible in the case of the smaller Gaussian diameter, w_4. On the presented cross-sections the relative lowering of the amplitude of the third and higher diffraction orders can easily be observed.

The numeric values of the area integrals allow for a more precise comparison. Even at a first glance, a trend among the Gaussian masks is rather visible, with monotonous decrease of the amplitude of third and fourth diffraction orders, and increase of the first diffraction order, that is, the amplitude of the main image. The notable increase in the second order of diffraction is, however, undesired. Yet, it could be reduced by the means of spatial filtering - combining the state of art technology with the method suggested in this paper could result in the increase of the intensity of the main image.

It is therefore crucial to analyse the normalized percentage distribution of the amplitude in respective diffraction orders, as presented in the Table 2. As expected, the trend of decreasing amplitude integrals in the area of the first diffraction order is noticeable. Despite redirecting more percentage of light into the main image, the large part of the wavefront is blocked due to applying the amplitude mask. The decrease in the first order is as big as 41.5 percentage points (pp) between the un-apodized spatial light modulator and the Gaussian mask of the smallest diameter, w_4. However, for the third and fourth diffraction order the reduction is much more significant, coming close to 95 percentage points. Again, in the second order of diffraction an undesired rising tendency is observed, with the amplitude increasing even despite the light suppression by the amplitude mask.

It is worth noting that the numeric results for the sinusoidal mask are rather similar to those obtained with a Gaussian mask of $w_4 = 2.5\ \mu m$. In the case of amplitude percentage in the respective diffraction orders, the value of the third and fourth orders is slightly lower (by around 3 pp) and the main image is also somewhat stronger (0.5 pp increase of the amplitude value). The normalized amplitude show a decrease in both of these areas (both by around 4-5 pp) in comparison to the Gaussian mask of w_4. While the two analysed data sets prove the rise of the amplitude in the second diffraction order, the simplicity of application of this mask, as explained in the next section, is an advantage enough to consider the results satisfactory.

Despite the seemingly undesired effect on the second order of diffraction, which is as well the closest to the main image and therefore can strongly influence the quality of the image reconstruction from Fourier hologram, the apodization simulation has proven the possibility of changing the effective pixel shape. As

Table 1: Percentage of amplitude distribution in respective diffraction orders for different apodizing masks - result of the simulations.

Mask shape	1st order	2nd order	3rd & 4th order
No apodization	17,74%	15,76%	27,31%
Gaussian mask ($w_1 = 4\ \mu m$)	19,29%	22,08%	24,59%
Gaussian mask ($w_2 = 3{,}5\ \mu m$)	20,36%	28,30%	21,79%
Gaussian mask ($w_3 = 3\ \mu m$)	21,64%	39,26%	16,52%
Gaussian mask ($w_4 = 2{,}5\ \mu m$)	22,48%	55,51%	8,58%
Sinusoidal mask	22,99%	69,97%	5,34%

Table 2: Normalized percentage of the amplitude distribution in respective diffraction orders for different apodizing masks - result of the simulations.

Mask shape	1st order	2nd order	3rd & 4th order
No apodization	100%	100%	100%
Gaussian mask ($w_1 = 4\ \mu m$)	82,92%	106,84%	68,64%
Gaussian mask ($w_2 = 3{,}5\ \mu m$)	66,19%	103,60%	46,03%
Gaussian mask ($w_3 = 3\ \mu m$)	51,60%	105,37%	25,59%
Gaussian mask ($w_4 = 2{,}5\ \mu m$)	38,50%	107,03%	9,54%
Sinusoidal mask	33,38%	114,40%	5,04%

predicted, the amplitude masks allowed a change of the distribution of the reconstructed images and while the results obtained are not yet ideal for the proposed purpose, the conducted research creates the possibility of optimising the masks parameters. Additionally, displaying the image in between the intensity peaks of main diffraction orders with the use of a carrier-frequency would have the advantage of increasing reconstruction efficiency with the observed gain of intensity in both first and second order of diffraction.

5 EXPERIMENT

The simulations are the first step of confirming the postulated hypothesis and because of the limitations of theoretical models, experimental proof is favourable. Especially the sinusoidal mask presents the greatest opportunity of experimental application due to its structure. In this paper we name a few of the possible application approaches.

The simplest of them would be mask fabrication and its positioning by the SLM surface in the set-up analogous to the one presented in Figure 1. It should be noted, however, that in such case the wavefront propagates twice through the amplitude mask. The shape of the mask should be then corrected. Using the Talbot self-imaging length could eliminate said obstacle, with the periodic structure reconstruction, up to a constant multiple, at a distance. The mask itself can be created precisely by the means of electrolitography or, in a simplistic case, by recording a hologram of an interference pattern of two plane waves, creating a sinusoidal structure in one of the dimensions. In the latter instance, care should be taken to accurately apply the correct angle between the waves. Another possible approach to the spatial light modulator apodization is a direct interference of two waves on the SLM plane.

6 SUMMARY

In this work, a solution to the intensity leakage in the image reconstruction of the computer-generated Fourier hologram was proposed. The higher diffraction orders are one of the reasons for the intensity decrease of the main image, thus we proposed the effective change of the pixel shape to reduce this effect. The apodizing structures described in this paper, that is Gaussian and sinusoidal masks, are not necessarily optimal for this purpose, however, intensity redirection to lower diffraction orders was still observed. It is a common practice to display the image off-axis with the use of holographic diffraction gratings, thus the final projection can benefit from the obtained intensity raise of both first and second orders.

Conducted simulations support the hypothesis that it is possible and relatively uncomplicated to alter the obtained amplitude distribution by the use of the amplitude mask, and control the change by modifying parameters of the mask. In order to analyse both masks of different shapes and experimental results for the simulated data, further study of the subject is necessary.

REFERENCES

Agour, M. et al. (2009). Suppression of higher diffraction orders and intensity improvement of optically reconstructed holograms from a spatial light modulator. In *Journal of Optics A: Pure and Applied Optics, 11(10), 105405, 120-128*.

Betin, A. Y. et al. (2013). Holographic memory optical system based on computer-generated fourier holograms. In *Applied Optics 52, 8142-8145*.

Casasent, D. (1977). Spatial light modulators. In *Proceedings of the IEEE, 65(1), 143-157*.

Denisiuk, I. N. (1978). Holography. In *Optiko Mekhanicheskaia Promyshlennost, 45, 9-13*.

Gabor, D. (1949). Microscopy by reconstructed wavefronts. In *Proceedings of the Royal Society of London A: Mathematical, Physical and Engineering Sciences, Vol. 197, No. 1051, pp. 454-487*. The Royal Society.

Kreyszig, E. (1988). *Engineering mathematics*. Wiley, 10th edition.

Makowski, M. et al. (2012). Simple holographic projection in color. In *Optics express, 20(22), 25130-25136*.

Meltaus, J. et al. (2003). Millimeter-wave beam shaping using holograms. In *IEEE Transactions on Microwave Theory and Techniques, 51(4), 1274-1280*.

Michakiewicz, A. and Kujawiska, M. (2009). Optoelectronic reconstruction of digital holograms. In *Elektronika: konstrukcje, technologie, zastosowania, 50(1), 120-128*.

Parker, M. C., Cohen, A. D., and Mears, R. J. (1997). Dynamic holographic spectral equalization for wdm. In *IEEE Photonics Technology Letters, 9(4), 529-531*.

Reicherter, M. et al. (1999). Optical particle trapping with computer-generated holograms written on a liquid-crystal display. In *Optics Letters, 24, 608-610*.

Slinger, C., Cameron, C., and Stanley, M. (2005). Computer-generated holography as a generic display technology. In *Computer, 38(8), 46-53*.

West, P. A. (1976). Holography in medicine. In *Journal of Modern Optics, 23(10), 845-845*.

Wolfke, M. (1920). Uber die moglichkeit der optischen abbildung von molekulargittern. In *Physikische Zeitschrft, 21, 495-7*.

Yang, H. et al. (2013). Origin of transient crosstalk and its reduction in phase-only lcos wavelength selective switches. In *Journal of Lightwave Technology, 31(23), 3822-3829*.

Yaras, F., Kang, H., and Onural, L. (2010). State of the art in holographic displays: a survey. In *Journal of display technology 6(10), 443-454*.

SCITEPRESS SCIENCE AND TECHNOLOGY PUBLICATIONS